

Fluorine-doped carbon coated $\text{LiFePO}_4\text{F}_x$ composites as cathode materials for high-performance lithium-ion batteries

Zhixiong Yan^{a,b}, Dequan Huang^{a,b}, Xiaoping Fan^{a,b}, Fenghua Zheng^{a,b,*}, Qichang Pan^{a,b}, Zhaoling Ma^{a,b}, Hongqiang Wang^{a,b}, Youguo Huang^{a,b}, Qingyu Li^{a,b,*}

^a School of Chemical and Pharmaceutical Sciences, Guangxi Normal University, Guilin, 541004, China

^b Guangxi Key Laboratory of Low Carbon Energy Materials, Guangxi Normal University, Guilin, 541004, China

E-mail addresses: zhengfh870627@163.com (F. Zheng); liqingyu62@126.com (Q. Li).

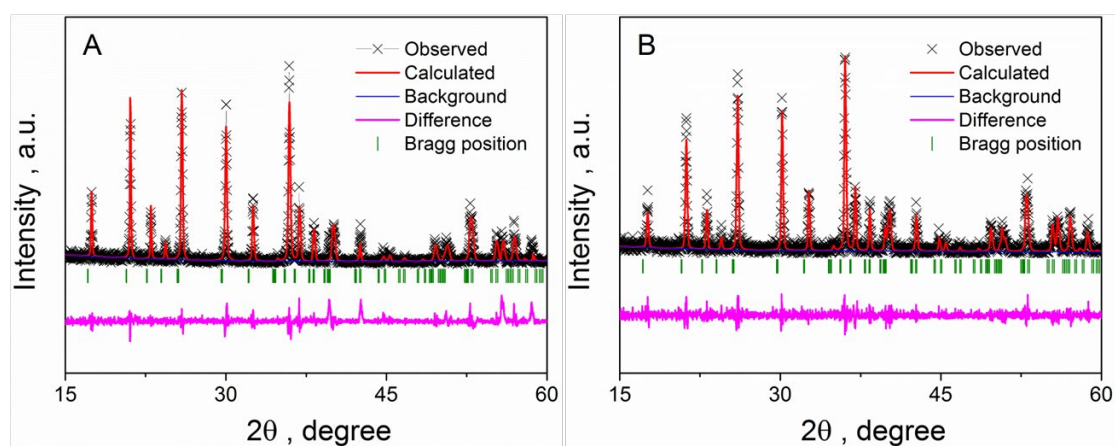


Fig. S1. Rietveld refinement plot of pure LFP and LFP/C, respectively.

Table S1. The lattice parameter and carbon content of pure LFP, LFP/C and LFPF/CF, respectively.

Samples	Lattice Parameters		
	a/Å	b/Å	c/Å
Pure LFP	6.0192	10.3375	4.7123
LFP/C	6.0188	10.3372	4.7120
LFPF/CF	6.0012	10.2212	4.2853

Table S2. The tap density of pure LFP, LFP/C and LFPF/CF composite, respectively.

Samples	Tap density(g/cm ³)
Pure LFP	1.25
LFP/C	1.22
LFPF/CF	1.20

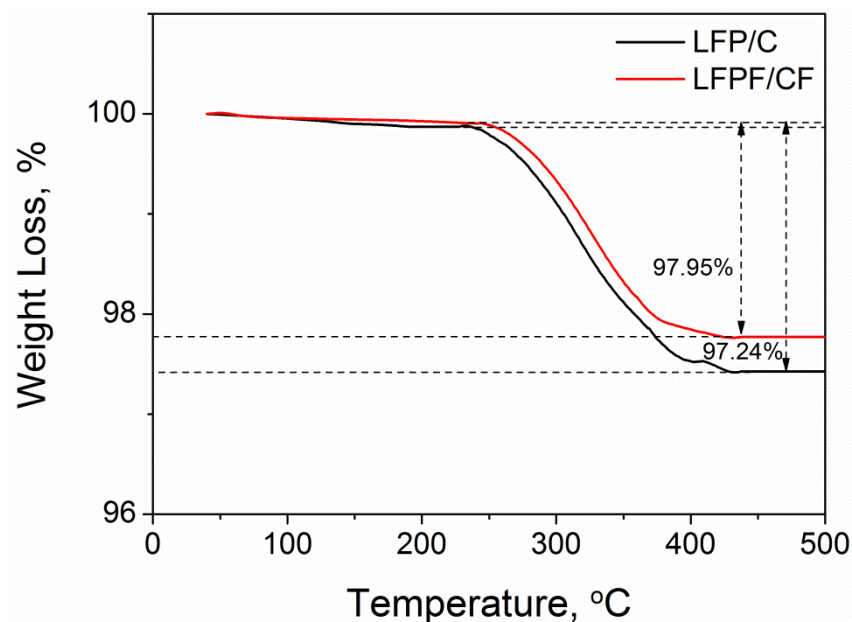


Fig. S2. TGA curves of LFP/C and LFPF/CF composite, respectively.

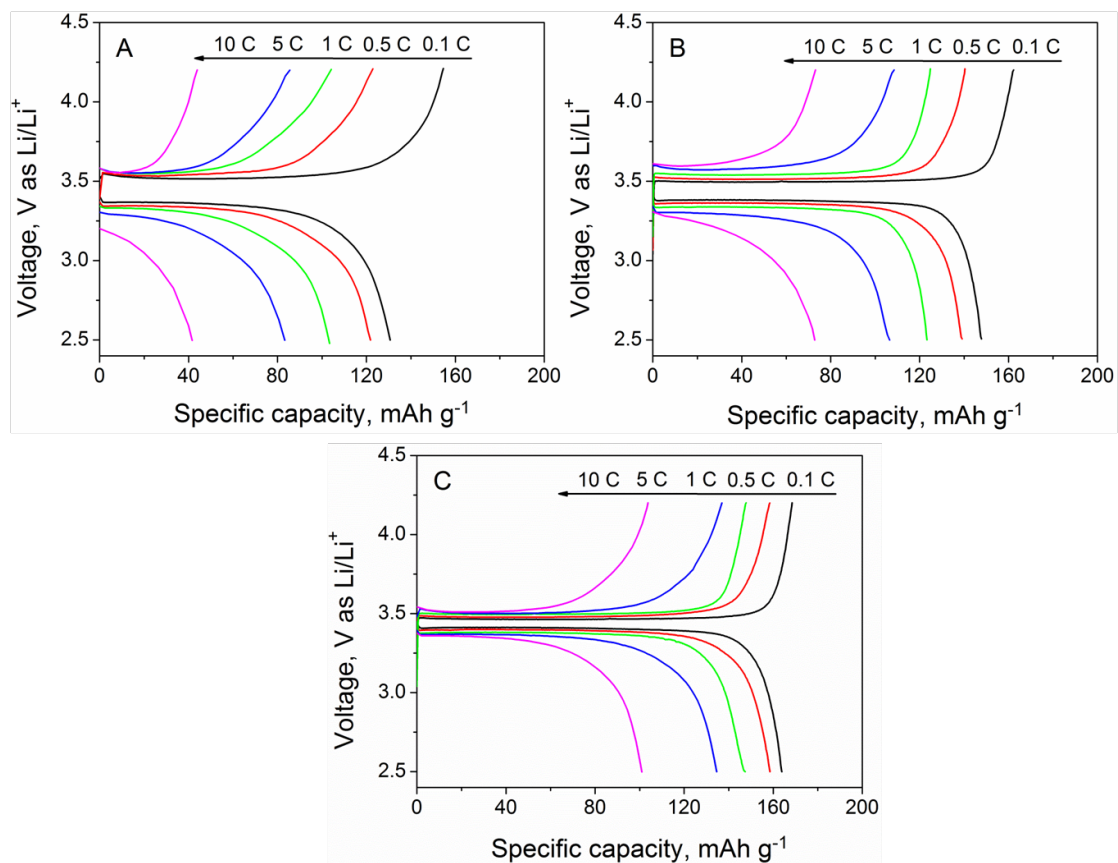


Fig. S3. The charge/discharge curves for pure LFP, LFP/C and LFP/CF composite at various rates of 0.1, 0.5, 1, 5 and 10 C, respectively.

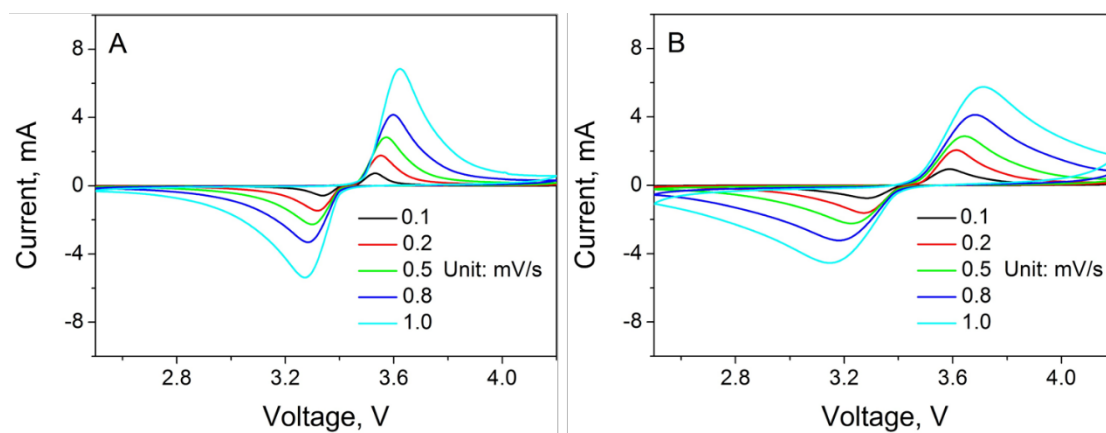


Fig. S4. The CV curves of pure LFP and LFP/C composites at different scanning rates.

Table S3. Impedance parameters obtained from equivalent circuit model (Fig. 8E) for pure LFP, LFP/C and LFPF/CF electrodes before cycling (fully discharged).

Before cycling			
Samples	Pure LFP	LFP/C	LFPF/CF
R_{Ω}/Ω	5.5	5.1	4.8
R_{ct}/Ω	558.8	339.2	178.6
$D_{Li^+} (\text{cm}^2\text{s}^{-1})$	0.87×10^{-12}	1.43×10^{-12}	2.72×10^{-12}

Table S4. Impedance parameters achieved from equivalent circuit model (Fig. 10E) for pure LFP, LFP/C and LFPF/CF electrodes after cycling (fully discharged).

Samples	Pure LFP			LFP/C			LFPF/CF		
	R_{Ω}/Ω	R_{ct}/Ω	$D_{Li^+} / \text{cm}^2\text{s}^{-1}$	R_{Ω}/Ω	R_{ct}/Ω	$D_{Li^+} / \text{cm}^2\text{s}^{-1}$	R_{Ω}/Ω	R_{ct}/Ω	$D_{Li^+} / \text{cm}^2\text{s}^{-1}$
1st	6.1	629.8	0.77×10^{-12}	5.5	402.2	1.21×10^{-12}	5.1	196.5	2.47×10^{-12}
300th	6.8	975.8	0.52×10^{-12}	6.2	534.6	0.91×10^{-12}	5.5	254.7	1.91×10^{-12}
500th	7.6	1372.9	0.35×10^{-12}	6.7	704.5	0.69×10^{-12}	5.8	314.8	1.54×10^{-12}

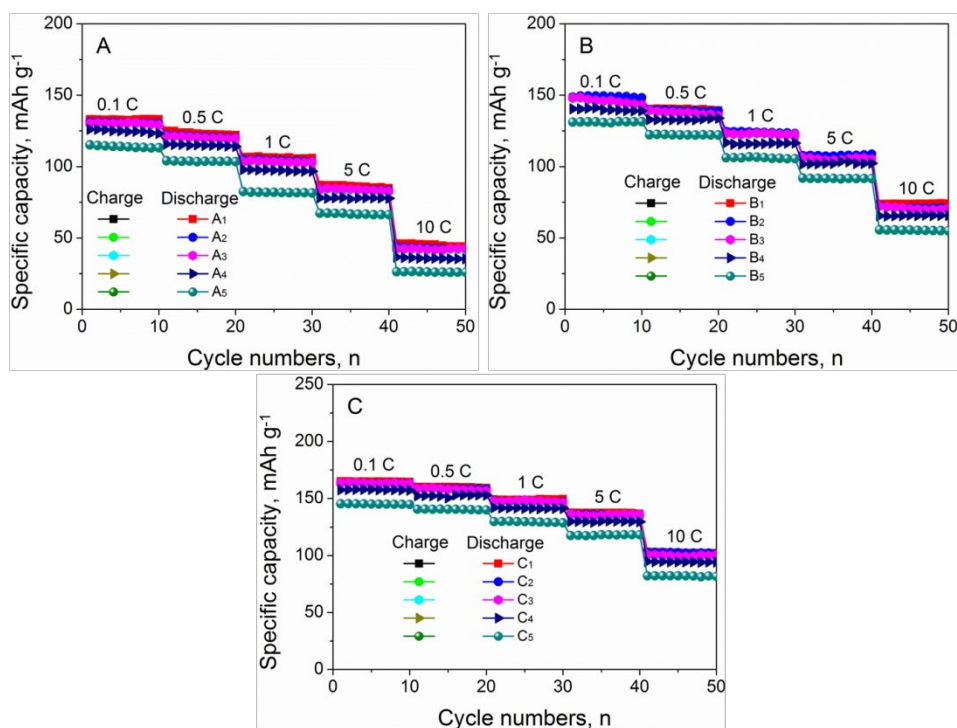


Fig. S5 Rate performance of pure LFP, LFP/C and LFPF/CF composite with different about mass loading of active cathode (A_1, B_1, C_1) 1.0 mg cm^{-2} , (A_2, B_2, C_2) 2.0 mg cm^{-2} , (A_3, B_3, C_3) 3.0 mg cm^{-2} , (A_4, B_4, C_4) 4.0 mg cm^{-2} , (A_5, B_5, C_5) 5.0 mg cm^{-2}

The different mass loading of the active material exhibit different electrochemical performance, as shown in Fig. S7. It is obvious seen that the electrochemical performance not vary much in the rang of $1.0\text{-}3.0 \text{ mg cm}^{-2}$. However, the electrochemical performance is slightly decline when the mass loading reach to $4.0\text{-}5.0 \text{ mg cm}^{-2}$, because of the increased electrochemical polarization during charge and discharge. Hence, the optimal mass loading of $1.0\text{-}3.0 \text{ mg cm}^{-2}$ were chosen in the follow-up investigation^[S1-S3].

[S1] Sun, H., Mei, L., Liang, J., Zhao, Z., Lee, C., Fei, H., Xu, X. (2017). Three-dimensional holey-graphene/niobia composite architectures for ultrahigh-rate energy storage. *Science*, 356(6338), 599-604. doi: 10.1126/science.aam5852

[S2] Wang, B., Al Abdulla, W., Wang, D., Zhao, X. S. (2015). A three-dimensional porous LiFePO_4 cathode material modified with a nitrogen-doped graphene aerogel for high-power lithium ion batteries. *Energy & Environmental Science*, 8(3), 869-875. doi.org/10.1039/c4ee03825h

[S3] Wang, B., Xie, Y., Liu, T., Luo, H., Wang, B., Wang, C., & Zhou, Y. (2017). LiFePO_4 quantum-dots composite synthesized by a general microreactor strategy

for ultra-high-rate lithium ion batteries. *Nano Energy*, 42, 363-372.
doi.org/10.1016/j.nanoen.2017.11.040

Table S5. The x value, F content of F-doped carbon layer and the amount of carbon content LFPF/CF composites from XPS analysis.

Sample	Mass ratios (Tween80 : PVDF)	x value	Carbon content/%	Fluorine content in the carbon layer/%
a	2:0.15	0.025	1.03	0.121
b	2:0.30	0.038	1.21	0.312
c	2:0.45	0.046	1.53	0.431
d	2:0.60	0.062	1.85	0.612
e	2:0.75	0.078	2.34	0.863

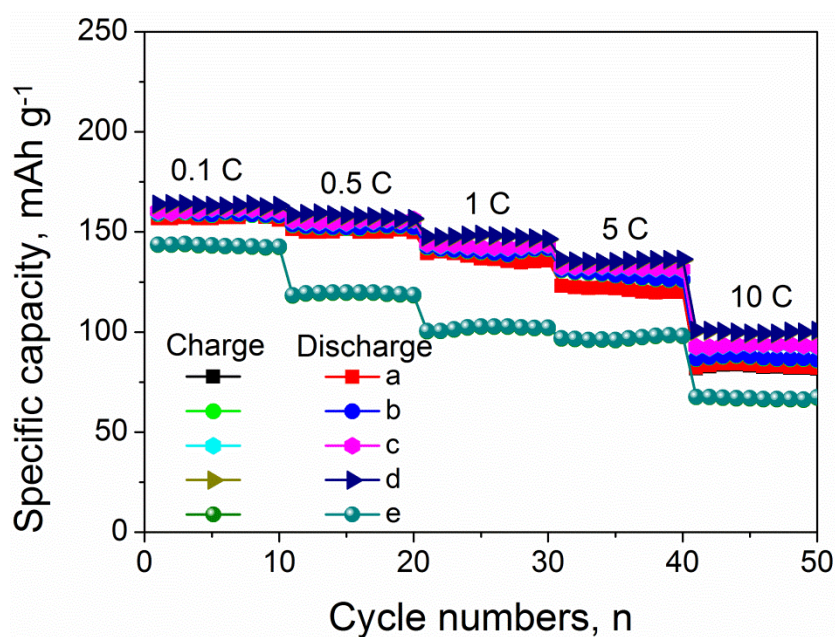


Fig. S6. Rate performance for LFPF/CF composite in different mass ratio of Tween40 and PVDF. (a 2:0.15, b 2:0.30, c 2:0.45, 2:0.60 and 2:0.75)

The fluorine content and carbon content in the LFPF/CF composite are determined by mass ratios of Tween40 and PVDF. To confirm the optimal x value, F content of F-doped carbon layer and the amount of carbon content in the LFPF/CF, a series of composite electrodes synthesized with mass ratios of Tween40 and PVDF.

The x value, F content in carbon layer and the amount of carbon content can be calculated by the XPS analysis, and the results listed in Table S5. In addition, the corresponding electrochemical measurements of LFPF/CF composite with different x value, F content of F-doped carbon layer and the amount of carbon content were conducted, as shown in Fig. S6. The electrochemical performance enhanced with the increase of x value, F content of F-doped carbon layer and the amount of carbon content. This phenomenon is caused by the following aspects: firstly, the crystal lattice of LFP was enlarged by the F doping, which facilitates the Li⁺ intercalation/deintercalation. Secondly, more fluorine doped carbon could provide more active sites for Li intercalation and form stronger electronic coupling between F-doped carbon and LFP. Thirdly, more carbon content increase the electrical conductivity of the interface. However, when x value, F content of F-doped carbon layer and the amount of carbon content reach to 0.078, 0.863% and 2.34%, the LFPF/CF show poor electrochemical performance. It is attributed to a large number of PVDF could produce a large amount of gas containing fluoride in the sintering process, resulting in more fluorine doped into LFP lattice and the carbon layer. Meanwhile, a large amount of containing fluoride damaged the particles surface and form large amount of fluoride, resulting in the consumption of lithium ion and high interfacial cell impedance. In addition, the higher carbon content increases the diffusion path of lithium ion, leading to poor rate performance. According to the rate property test, it shows that x value, F content of F-doped carbon layer and the amount of carbon content with 0.062, 0.612% and 1.85% demonstrates the best performance. For example, the discharge capacities reach to 163.4, 158.3, 147.2, 136.3 and 100.6 mA h g⁻¹ at 0.1, 0.5, 1, 5 and 10 C, respectively. Therefore, x value, F content of F-doped carbon layer and the amount of carbon content with 0.062, 0.612% and 1.85% are the optimal content, and the corresponding electrode exhibits the best electrochemical performance. Hence, the optimal x value, F content of F-doped carbon layer and the amount of carbon content were chosen in the follow-up investigation.